# Single-photon multiple ionization of neon in the *K*-edge region

D. V. Morgan,[1] M. Sagurton,[2] and R. J. Bartlett[1]
[1]*Los Alamos National Laboratory, Los Alamos, New Mexico 87545*
[2]*Los Alamos National Laboratory/SFA, NSLS, Building 725-X8, Brookhaven National Laboratory, Upton, New York 11973*
(Received 6 September 1996)

The ion charge state yields resulting from the photoionization of neon gas have been measured with time-of-flight ion charge state spectroscopy for excitation energies in the *K*-edge region. The decay of the $[1s]3p$ resonance excited state results in the formation ion charge states $Ne^{+}$, $Ne^{2+}$, $Ne^{3+}$, and $Ne^{4+}$, with a branching ratio of 0.65:0.32:0.030:0.002, whereas the final charge state for the decay of higher-order $[1s]np(n\geq 4)$ and $[1s]\varepsilon p$ continuum excitations is mostly $Ne^{2+}$. We have measured $\overline{q}$, the mean charge from photoionization, for excited states near the *K* edge as a function of photon energy. Postcollision interaction effects are shown to be quite small. [S1050-2947(97)05802-2]

PACS number(s): 32.80.Fb, 32.80.Rm

Monochromatic x-ray photoexcitation of closed-shell, monatomic, inert gases (such as neon) provides a method by which inner-shell effects and electron-electron interactions may be studied. With sufficient photon excitation energy, inner-shell vacancies are produced by photoelectric excitation, and at photon energies several tens of eV above the inner-shell absorption edge, an interaction between the escaping photoelectron and valence electrons may occur, resulting in a multiple-hole excited state. Electron-electron interactions may also occur during the decay of the inner-shell hole. For example, Auger shakeoff and Auger shakeup may occur as a result of an interaction between an escaping Auger electron and a valence electron. The decay of these single- and multiple-hole excited states through a set of distinct processes results in a distribution of final ion charge states that depends on the photon excitation energy and the photoexcited state. Monochromatic synchrotron radiation allows energy selective excitation of states, which is especially important near the absorption edge, and the high intensity of these sources enables us to observe interactions that occur with very low probability. Neon *K*-shell photoexcitation is of interest because only a limited number of decay paths are possible for this simple two-shell system, compared with high-*Z* atoms. In fact, for $[1s]\varepsilon p$ $\varepsilon \gg 0$ excitations, each decay path is uniquely associated with one final ion charge state. The complications in the ion charge state spectra that occur for $[1s]np$ and $[1s]\varepsilon p$ $\varepsilon \gtrsim 0$ excitations are the topic of this paper.

The photoionization ion charge state spectra of neon have been observed by Saito and Suzuki with time-of-flight (TOF) ion charge state spectroscopy for photon energies from 44 eV to 1.4 keV, including low-energy resolution experiments ($\lambda/\Delta\lambda \approx 200$) in the *K*-edge region [1–3]. Below the neon *K* edge, valence electron photoionization produces mostly singly charged $Ne^{+}$, with small fractional yields [3,4] of $Ne^{2+}$($\approx$14%) and $Ne^{3+}$($\approx$1.0%). Above the *K* edge, Auger decay of the $[1s]\varepsilon p$ excited state results primarily in the formation of $Ne^{2+}$ through normal Auger decay of the *K* hole, with smaller fractional yields of $Ne^{3+}$ and $Ne^{4+}$ formed as the result of Auger shakeoff. At photon energies just below the neon $[1s]\varepsilon p$ excitation threshold, the photoelectron may be excited into $[1s]np$ Rydberg states. The structures of the neon $[1s]3p$, $[1s]4p$ resonance peaks and the $[1s]\varepsilon p$ continuum excitations have been well documented by x-ray photoabsorption spectroscopy [5–7]. In the case of $[1s]np$ resonance excitations, the photoelectron may be ejected by Auger shakeoff, or by autoionization of the $[2s^2]np$ or $[2s2p]np$ decay states formed after the initial $K$-$L_1L_1$ and $K$-$L_1L_{2,3}$ decays, the so-called ''two-step'' process. According to the recent result of Hayaishi *et al.* [8], the states $[2p^2]np, n\geq 4$ may also have sufficient energy to autoionize, forming a $Ne^{2+}$ final charge state. Aksela *et al.* [9] have observed Auger emission from the $[1s]3p$ excited states of neon with high-resolution electron spectroscopy, and have emphasized the importance of the $3p\rightarrow 4p$ shakeup satellites that occur during Auger deexcitation of the $[1s]3p$ excited state. They have also shown that the role of the $np$ electron as a participator in the *K*-shell Auger decay process is quite small, and that the $np$ electron may be retained by the ion as a spectator during the Auger decay. As the incident photon energies are increased through the neon *K*-edge region, the fractional yields of the ion charge states depend on whether the photoelectron is retained by the ion, shaken off, or involved in a two-step decay.

In this paper, we report the fractional yields of the neon ion charge states produced by photoionization in the *K*-edge region. The normalized total ion yield will be compared with existing photoabsorption spectra to determine the photoexcited states. For $[1s]np$ resonance excitations, we shall determine the branching ratios for the final ion charge states, and compare these ratios with existing experimental and theoretical values. For $[1s]\varepsilon p$ continuum excitations, we shall characterize the postcollision interaction (PCI) effects by determining the mean charge, $\overline{q}$, as a function of photon energy above the *K* edge.

The X8A beam line at the Brookhaven National Synchrotron Light Source was used as a monochromatic photon source in the 860–900 eV energy range for this experiment, and has been described previously [10]. Two beryl (1010) crystals with a 15.93 Å $2d$ spacing [7] in a parallel configuration were used as the monochromator for this experiment. The upstream beryl monochromator crystal, despite water cooling, was found to be susceptible to thermal damage from

 

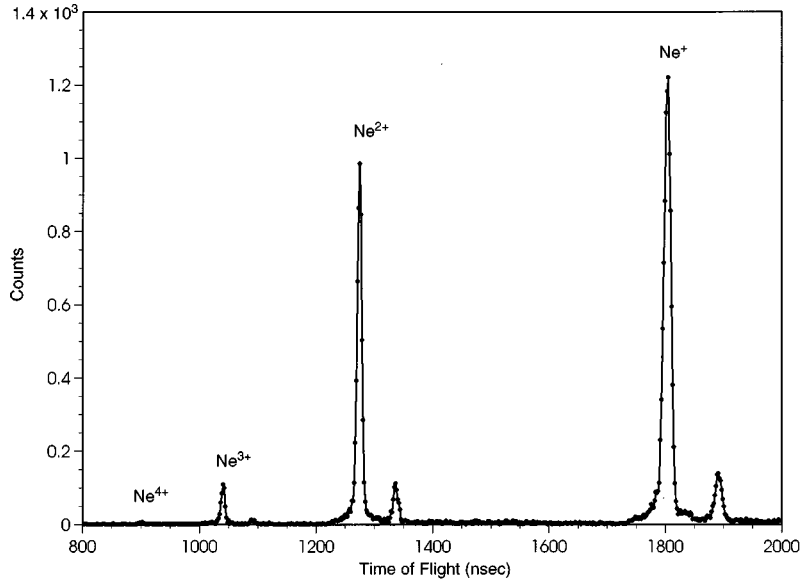


FIG. 1. Neon TOF spectrum at 867.3 eV corresponding to the $[1s]3p$ resonance excitation peak. The natural isotopic abundances are 90.5% $^{20}_{10}$Ne and 9.2% $^{22}_{10}$Ne.

high-intensity white synchrotron light, especially at large Bragg angles. This problem was overcome by blocking the intense, central portion of the beam with a vertically inserted, water-cooled aperture upstream from the monochromator, thereby utilizing the less intense beam fringe. Unfortunately, this resulted in a low count rate for this experiment. UV light was prevented from reaching the interaction region by a 10-$\mu$m Mg filter. The $K$-edge of the Mg filter at 1303 eV was also helpful for reducing second-order reflections from the beryl monochromator crystals for photon energies in the neon $K$-edge region.

A TOF ion charge state spectrometer, described previously [10], of the Wiley-McLaren variety [11] was used to obtain the ion charge state spectra. Neon gas was injected into the interaction region perpendicular to both the x-ray beam and the TOF instrument axis of symmetry by an effusive gas nozzle. Experiments were performed with the photon electric field polarization vector both parallel and perpendicular to the TOF axis of symmetry, but the effects on the experimental results were negligible. The ambient sample gas pressure in the sample chamber was maintained at $2.0\times10^{-6}$ torr, after the system had been evacuated to a base pressure in the low $10^{-9}$ torr range. Ions were extracted from the interaction region by a pulsed electric field with a 15-$\mu$sec pulse repetition time and a 520-nsec pulse width. The leading edge of the electric field pulse also served as the timing start pulse for the TOF system. After being extracted from the interaction region, the ions travel through a focusing acceleration region, a field-free drift region, and a post-acceleration region before being detected by the microchannel plate detector. The ion signal pulse from the detector generates a timing stop pulse for the TOF system. The ion charge states are thus separated according to their time of flight, which scales as the square root of the ion mass-to-charge ratio. Due to our low counting rate, the probability for observing two ions in a single pulse repetition interval was negligible, and no corrections were made. Precautions were taken to prevent electron impact ionization from contributing to the $Ne^+$ signal. Magnets were placed along the beamline both upstream and downstream from the sample chamber to deflect externally produced electrons away from the sample chamber, and successive upstream beam apertures effectively eliminated photoelectrons produced by scattered photons striking the TOF apparatus.

The TOF spectra at each photon energy were recorded in a data file in the computer pc, and the TOF spectrum at $h\nu=867.3$ eV corresponding with the $[1s]3p$ excitation is shown in Fig. 1. For each data file, the area under each ion charge state peak was determined, and the fractional yields for the ion charge states at each photon energy were calculated. A Monte Carlo simulation was performed to determine the necessary corrections for the slight variations in the collection efficiencies of the ion charge states due to the ion recoil velocities. This simulation program was also used to determine the corrections for overlap of the ion charge states in the TOF spectrum caused by ''late arrival'' ions created in the interaction region during the time that the extraction field was turned on. The ion yield data was normalized using an x-ray detector (XRD) at the end of the beamline to account for fluctuations in the x-ray beam intensity.

The experimental values for the $Ne^+$ and $Ne^{2+}$ ion charge state yields and the total ion yield as a function of photon energy are shown in Fig. 2. The total ion yield, as expected, appears quite similar to the spectrum observed by high-resolution x-ray photoabsorption experiments [5–7]. The $Ne^+$ yield dominates at the $[1s]3p$ resonance peak, and exhibits a smaller peak for $[1s]4p$ excitations, while the $Ne^{2+}$ yield is dominant for photon energies at and above the $[1s]4p$ resonance peak, which concurs with the results of Hayaishi *et al.* [8]. The $Ne^{3+}$ and $Ne^{4+}$ ionization states were also observed in the $K$-edge region, but these yields were much smaller. The data were accumulated over five separate energy scans, and the photon energies for each scan were calibrated such that the excitation energy of the $[1s]3p$ peak matched the accepted value of 867.3 eV [6]. We have neglected the slight variation in the XRD efficiency over the narrow photon energy range near the neon $K$ edge. The full width at half maximum (FWHM) for the $[1s]3p$ excitation peak in our total ion yield data was found to be

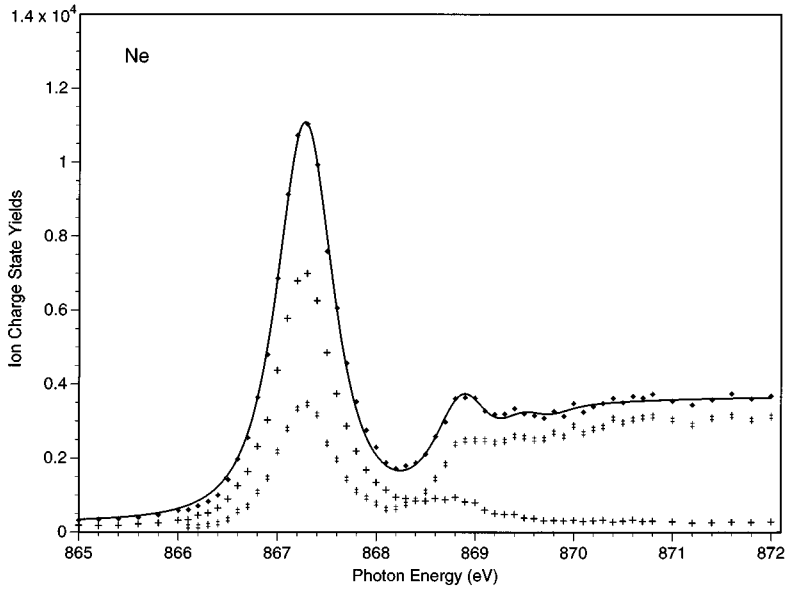


FIG. 2. Ion charge state yields as a function of photon energy in the neon $K$-edge region. ◆, total ion yield data; +, $Ne^+$ ion yield data; ≠, $Ne^{2+}$ ion yield data.

$0.67 \pm 0.03$ eV, while the natural line width of the $[1s]3p$ absorption line has been given by Oliver and Krause [12] as 0.24 eV. Because the natural line width is much less than the measured line width, we conclude that the photon energy distribution of our beamline monochromator was primarily responsible for the observed line width and structure.

For a given excited state in the neon $K$-edge region, the different decay pathways lead to a distribution of ion charge states and an associated mean charge $\overline{q}$. For $[1s]np$ excitations, the mean charge $\overline{q_{np}}$ depends heavily upon whether the $np$ electron is shaken off or otherwise removed during the decay. For $[1s]\varepsilon p$ continuum excitations just above the $K$ edge, where $\varepsilon$ is the energy above threshold, the mean charge $\overline{q_{\varepsilon p}}$ is generally less than $\overline{q_{\varepsilon p}}$ in the $\varepsilon \rightarrow \infty$ limit as the result of the postcollision interaction effect, where a slow moving photoelectron is recaptured by the ion due to an interaction with an escaping Auger electron. Determination of the $\overline{q_{np}}$ and $\overline{q_{\varepsilon p}}$ in the $K$-edge region is difficult because of the overlap in the excited states due to natural and instrumental line broadening. Therefore, suitable functions must be determined to approximate the absorption line shapes.

Over a narrow energy range, the $K$-edge absorption spectrum for neon may be represented by $\delta$ functions for the $[1s]np$ resonance excitations and with a step function for the $[1s]\varepsilon p$ continuum excitations, convoluted with the appropriate instrument and natural line broadening functions [10,13,14]. We have used a least-squares fit to represent the total ion yield spectrum with the sum of four functions representing the $[1s]3p$, $[1s]4p$, $[1s]5p$ resonance excitations, and $[1s]\varepsilon p$ continuum excitations. The representation of the unresolvable Rydberg states $[1s]np$ $(n \geqslant 6)$, may be simplified utilizing the recent analysis of Teodorescu *et al.* [15], where the continuum threshold energy is reduced to a lower ''apparent'' threshold, and the unresolved, high-order $(n \geqslant 6)$ Rydberg states are treated as part of the continuum. The values cited by Teodorescu *et al.* [15] for the energy

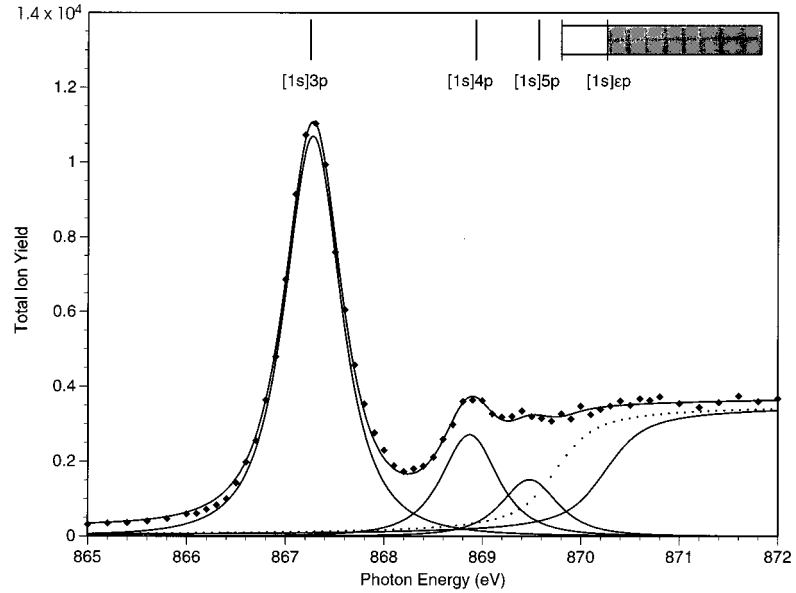


FIG. 3. Least-squares approximation to the ion yield data. The dotted curve represents the lowering of the continuum threshold 0.5 eV to an ''apparent'' threshold to account for the unresolved, high-order Rydberg states, $[1s]np$, $n \geqslant 6$.

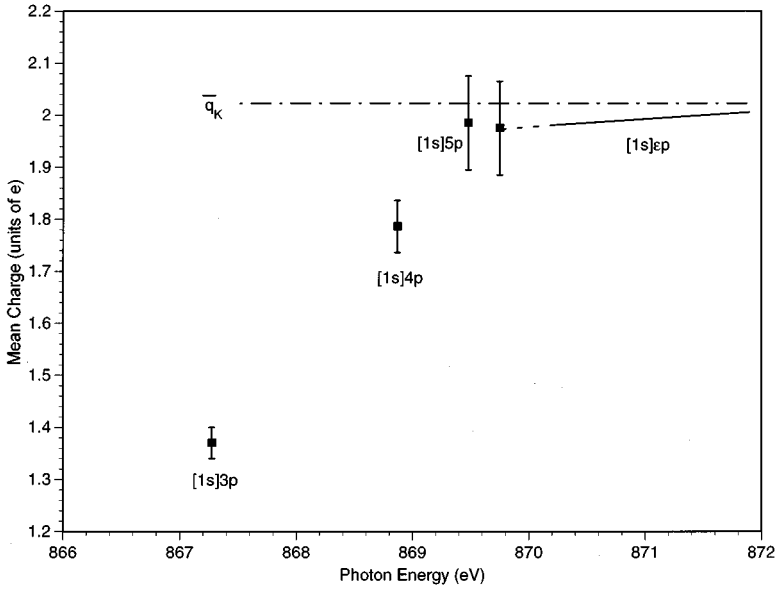


FIG. 4. Mean charge from photoionization as a function of photon energy. The solid line indicates the experimental values for the mean charge for continuum excitations, $\overline{q_{\varepsilon p}}$, above the $[1s]\varepsilon p$ threshold. The dotted line shows our approximation for the mean charge for the unresolved high-order Rydberg $[1s]np$ ($n \geq 6$) excitations. The dot-dashed line represents the asymptotic value for the mean charge for $[1s]\varepsilon p$ excitations in the limit $\varepsilon \rightarrow \infty$, $\overline{q_K}$.

separation of each of the resolvable Rydberg states and ''apparent'' edge have been used in our analysis. The least-squares approximation to the total ion yield data is shown as the solid line in Fig. 3. The contributions due to $L$-shell photoexcitation have been accounted for by extrapolation of the photoabsorption cross section data given by Marr and West [16] above and below the neon $K$ edge. From this data, we have estimated the ratio for the $K$-shell photoionization cross section to the $L$-shell photoionization cross section to be 14.5 just above the $K$ edge. The variations in the $L$-shell cross section are very small over the energy range shown in Fig. 3, and have been neglected.

The experimental mean ion charge from photoionization, $\overline{q(h\nu)}$, in the $K$-edge region can be represented by an average of the $\overline{q_{np}}$, $\overline{q_{\varepsilon p}}$, and $\overline{q_L}$, weighted by their associated line broadened cross sections [10,17]. This is given as

$$\overline{q(h\nu)} = \frac{\overline{q_L}\sigma_L + \sum_{n=3}^{5} \overline{q_{np}}\sigma_{np}(h\nu) + \int_0^{\infty} \overline{q_{\varepsilon' p}}\sigma_{\varepsilon' p}(h\nu)\,d\varepsilon'}{\sum_{n=K,L} \sigma_n}, \quad (1)$$

where $\overline{q_L} = 1.16$ in units of $e$ is the mean charge for $L$-shell photoexcitation [3,4], $\overline{q_{np}}$ is the mean charge for $[1s]np$ Rydberg excitations, $\overline{q_{\varepsilon' p}}$ is the mean charge for continuum excitations at $\varepsilon'$, the energy above the ''apparent'' threshold, and $\sigma_L$, $\sigma_{np}(h\nu)$, and $\sigma_{\varepsilon' p}$ represent the line broadened photoionization cross sections. The ''apparent'' continuum threshold lies 0.5 eV below the actual $[1s]\varepsilon p$ threshold at 870.3 eV [6–15], i.e., $\varepsilon' - \varepsilon = 0.5$ eV. A least-squares fit was performed to determine the parameters $\overline{q_{3p}}$, $\overline{q_{4p}}$, $\overline{q_{5p}}$, and $\overline{q_{\varepsilon' p}}$ in Eq. (1) so that the values for $\overline{q(h\nu)}$ in Eq. (1) match the experimental values. This procedure has been described previously in greater detail [10]. The values for $\overline{q_{\varepsilon p}}$ determined from the least-squares fit are shown in Fig. 4. The value for $\overline{q_{\varepsilon p}}$ for $[1s]\varepsilon p$ excitations in the limit $\varepsilon \rightarrow \infty$ (henceforth referred to as $\overline{q_K}$) was found to be $2.03 \pm 0.03$ in units $e$. This value was determined from the ion charge state yields at a photon energy of 895 eV, which is below the $K$-$L$ double photoexcitation threshold, but above possible $K$ edge PCI effects. For $[1s]\varepsilon p$ continuum excitations near the $K$ edge, the mean charge is observed to be close to the value of $\overline{q_K}$ within experimental uncertainty, indicating that PCI effects are quite small. The values for $\overline{q_{3p}}$ and $\overline{q_{4p}}$ are given in Table I, along with the ion charge

TABLE I. Comparison of the fractional ion yields for the $[1s]3p$ and $[1s]4p$ resonance excitations.

| | Excited state $[1s]3p$ | | | $[1s]4p$ | |
|---|---|---|---|---|---|
| Ion charge state | This work | Hayashi *et al.* [a] | Omar and Hahn [b] | This work | Hayashi *et al.* [a] |
| $Ne^+$ | $0.65 \pm 0.02$ | 0.64 | 0.598 | $0.24 \pm 0.03$ | 0.22 |
| $Ne^{2+}$ | $0.32 \pm 0.02$ | 0.33 | 0.401 | $0.71 \pm 0.04$ | 0.73 |
| $Ne^{3+}$ | $0.03 \pm 0.01$ | 0.03 | | $0.04 \pm 0.01$ | 0.05 |
| $Ne^{4+}$ | (0.002) | | | (0.002) | |
| $\overline{q}$ (units of $e$) | $1.37 \pm 0.03$ | 1.39 | 1.400 | $1.78 \pm 0.05$ | 1.83 |

[a]Reference [8]
[b]Reference [18].

TABLE II. Comparison of the fractional ion yields for the $[1s]\varepsilon p$ continuum excitations in the limit $\varepsilon\rightarrow\infty$.

| | $[1s]\varepsilon p$, $\varepsilon\rightarrow\infty$ | | | | | |
|---|---|---|---|---|---|---|
| | Experiment | | | Theory | | |
| Ion charge state | This work | Saito and Suzuki [a] | Hayaishi *et al.* [b] | Kochur *et al.* [c] | Omar and Hahn [d] | Amusia *et al.* [e] |
| $Ne^{+}$ | $0.015\pm0.003$ | | | 0.013 | 0.0158 | |
| $Ne^{2+}$ | $0.935\pm0.004$ | 0.939 | | 0.980 | 0.9426 | |
| $Ne^{3+}$ | $0.048\pm0.002$ | 0.058 | | 0.007 | 0.0390 | |
| $Ne^{4+}$ | $0.003\pm0.001$ | 0.003 | | | 0.0026 | |
| $Ne^{3+}/Ne^{2+}$ | $0.051\pm0.004$ | 0.06 | 0.07 | | 0.0414 | 0.042 |

[a]Reference [1], corrected to exclude $L$-shell ionization.
[b]Reference [8].
[c]Reference [20].
[d]Reference [19].
[e]M. Ya. Amusia, I. S. lee, and V. A. Kilin, Phys. Rev. A **45**, 4576 (1992).

state fractional yields for the $[1s]3p$, $[1s]4p$ resonance excitation states and the $[1s]\varepsilon p$ continuum state in the $\varepsilon\rightarrow\infty$ limit. Our experimental values for the ion charge state fractional yields following $[1s]3p$ and $[1s]4p$ excitations are in good agreement with the recent results of Hayaishi *et al.* [8]. However, for $[1s]3p$ excitations, considerable disparity exists between the experimental results for the ion charge state fractional yields and the theoretical values given by Omar and Hahn [18], which exclude shakeoff effects.

It has been demonstrated that the $[2s^2]$ state of neon formed after the $K$-$L_1L_1$ Auger decay of the $K$-hole vacancy has insufficient energy to autoionize and form a $Ne^{3+}$ final charge state [1]. Therefore, each ion charge state formed following decay of the $[1s]\varepsilon p$ excitations in the $\varepsilon\rightarrow\infty$ limit is associated with a single decay path. Singly ionized $Ne^{+}$ ions are formed as the result of $K\alpha$ x-ray emission, and $Ne^{2+}$ is formed following normal $K$-$LL$ Auger decay. $Ne^{3+}$ and $Ne^{4+}$ are formed as the result of double ($K$-$LLL$) and triple ($K$-$LLLL$) Auger decay, respectively. The ratio of the fractional yields of $Ne^{3+}$ to $Ne^{2+}$ for $[1s]\varepsilon p$ excitations in the $\varepsilon\rightarrow\infty$ limit gives an indication of the probability for shakeoff to occur during Auger decay. A comparison of theoretical and experimental values for the ratio of $Ne^{3+}/Ne^{2+}$ for $[1s]\varepsilon p$ excitations in the $\varepsilon\rightarrow\infty$ limit is given in Table II. Our values for the branching ratios for the ion charge states in Table II are in good agreement with both the experimental values of Saito and Suzuki [1] and the theoretical values of Omar and Hahn [19]. The values for these branching ratios given by Kochur *et al.* [20] exclude shakeoff effects. Our experimental value for the fractional yield of the $Ne^{+}$ charge state for $[1s]\varepsilon p$ excitations in the $\varepsilon\rightarrow\infty$ limit shown in Table II agrees closely with the value of 0.0159 given for the $[1s]$ fluorescence yield cited by Chen and Crasemann [21].

In conclusion, we have observed the ion charge state spectra resulting from the photoionization of neon gas as a function of photon energy in the $K$ edge region. The photoexcited states have been distinguished by a least squares fit of the line broadened excitation states near the $K$ edge to the total ion yield data. We have determined the values for the mean charge from photoionization and the branching ratios for $[1s]3p$, $[1s]4p$, and $[1s]\varepsilon p$, $\varepsilon\rightarrow\infty$ excitations. Two eV above the $K$-edge, the mean charge was observed to differ from the asymptotic value by less than 0.02 units of $e$, indicating that PCI effects are quite small.

This material is based on work supported by the U.S. Department of Energy through Los Alamos National Laboratory.

[1] N. Saito and H. Suzuki, Phys. Scr. **45**, 253 (1992).
[2] N. Saito and H. Suzuki, Phys. Scr. **49**, 80 (1994).
[3] N. Saito and H. Suzuki, Int. J. Mass Spectrom. Ion Process. **115**, 157 (1992).
[4] R. J. Bartlett, P. J. Walsh, Z. X. He, Y. Chung, E.-M. Lee, and J. A. R. Samson, Phys. Rev. A **46**, 5574 (1992).
[5] R. J. Liefeld, Appl. Phys. Lett. **7**, 276 (1965).
[6] F. Wuilleumier, J. Phys. (Paris) **32**, C4 (1971).
[7] J. M. Esteva, B. Gauthé, P. Dhez, and R. C. Karnatak, J. Phys. B **16**, L263 (1983).
[8] T. Hayaishi, E. Murakama, Y. Morioka, E. Shigemasa, A. Yagishita, and F. Koike, J. Phys. B **28**, 1411 (1995).
[9] H. Aksela, S. Aksela, J. Tullki, T. Åberg, G. M. Bancroft, and K. H. Tan, Phys. Rev. A **39**, 3401 (1989).
[10] D. V. Morgan, R. J. Bartlett, and M. Sagurton, Phys. Rev. A **51**, 2939 (1995).
[11] W. C. Wiley and I. H. McClaren, Rev. Sci. Instrum. **26**, 1150 (1955).
[12] M. O. Krause and J. H. Oliver, J. Phys. Chem. Ref. Data **8**, 329 (1979).
[13] M. Breinig, M. H. Chen, G. E. Ice, R. Parente, B. Crasemann, and G. S. Brown, Phys. Rev. A **22**, 520 (1980).
[14] L. G. Parratt, Phys. Rev. **56**, 295 (1939).
[15] C. M. Teodorescu R. C. Karnatak, J. M. Esteva, A. El Afif, and J.-P. Connerade, J. Phys. B **26**, 4019 (1993).

[16] G. V. Marr and J. B. West, At. Data Nucl. Data Tables **18**, 497 (1976).
[17] T. Tonuma, A. Yagishita, H. Shibata, T. Koizumi, T. Matsuo, K. Shima, T. Mukoyama, and H. Tawara, J. Phys. B **20**, L31 (1987).
[18] G. Omar and Y. Hahn, Phys. Rev. A **43**, 4695 (1991).
[19] G. Omar and Y. Hahn, Z. Phys. D **25**, 31 (1992).
[20] A. G. Kochur, V. L. Sukhorukov, A. I. Dudenko, and P. V. Demekhin, J. Phys. B **28**, 387 (1995).
[21] M. S. Chen and B. Crasemann, Phys. Rev. A **12**, 959 (1975).